



Oxygen isotope and ^{26}Al - ^{26}Mg systematics of aluminum-rich chondrules from unequilibrated enstatite chondrites

Yunbin GUAN^{1*}, Gary R. HUSS^{1, 2†}, Laurie A. LESHIN^{1, 2‡},
Glenn J. MACPHERSON³, and Kevin D. MCKEEGAN⁴

¹Department of Geological Sciences, Arizona State University, Tempe, Arizona 85287–1404, USA

²Center for Meteorite Studies, Arizona State University, Tempe, Arizona 85287–1404, USA

³Department of Mineral Sciences, National Museum of Natural History, Smithsonian Institution,
Washington, D.C. 20560–0119, USA

⁴Department of Earth and Space Sciences, University of California—Los Angeles, Los Angeles, California 90095–1567, USA

*Present address: University of Hawai‘i at Manoa, Hawai‘i Institute of Geophysics and Planetology,
1680 East-West Road, POST 602, Honolulu, Hawai‘i 96822, USA

††Present address: Sciences and Exploration Directorate, Code 600, NASA Goddard Space Flight Center, Greenbelt, Maryland 20771, USA

*Corresponding author. E-mail: yunbin.guan@asu.edu

(Received 31 January 2005; revision accepted 21 September 2005)

Abstract—Correlated in situ analyses of the oxygen and magnesium isotopic compositions of aluminum-rich chondrules from unequilibrated enstatite chondrites were obtained using an ion microprobe. Among eleven aluminum-rich chondrules and two plagioclase fragments measured for ^{26}Al - ^{26}Mg systematics, only one aluminum-rich chondrule contains excess ^{26}Mg from the in situ decay of ^{26}Al ; the inferred initial ratio ($^{26}\text{Al}/^{27}\text{Al}$)₀ = (6.8 ± 2.4) × 10⁻⁶ is consistent with ratios observed in chondrules from carbonaceous chondrites and unequilibrated ordinary chondrites.

The oxygen isotopic compositions of five aluminum-rich chondrules and one plagioclase fragment define a line of slope ~0.6 ± 0.1 on a three-oxygen-isotope diagram, overlapping the field defined by ferromagnesian chondrules in enstatite chondrites but extending to more ^{16}O -rich compositions with a range in $\delta^{18}\text{O}$ of about ~12‰. Based on their oxygen isotopic compositions, aluminum-rich chondrules in unequilibrated enstatite chondrites are probably genetically related to ferromagnesian chondrules and are not simple mixtures of materials from ferromagnesian chondrules and calcium-aluminum-rich inclusions (CAIs).

Relative to their counterparts from unequilibrated ordinary chondrites, aluminum-rich chondrules from unequilibrated enstatite chondrites show a narrower oxygen isotopic range and much less resolvable excess ^{26}Mg from the in situ decay of ^{26}Al , probably resulting from higher degrees of equilibration and isotopic exchange during post-crystallization metamorphism. However, the presence of ^{26}Al -bearing chondrules within the primitive ordinary, carbonaceous, and now enstatite chondrites suggests that ^{26}Al was at least approximately homogeneously distributed across the chondrite-forming region.

INTRODUCTION

Aluminum-rich chondrules are rare components in most primitive chondrites and contain one or more of the primary phases plagioclase, spinel, and aluminous diopside, ±aluminum-rich glass, in addition to olivine and calcium-poor pyroxene. Because the plagioclase and glass commonly have suitably high Al/Mg ratios for in situ analysis by ion microprobe, aluminum-rich chondrules are important candidates in the search for extinct ^{26}Al (e.g., Russell et al.

1996; Kita et al. 2000; Huss et al. 2001). In addition, petrologic and oxygen isotopic studies of aluminum-rich chondrules in carbonaceous and ordinary chondrites (Russell et al. 2000; Krot and Keil 2002; Krot et al. 2004; MacPherson and Huss 2005) hint that these chondrules may represent a transitional link between calcium-aluminum-rich inclusions (CAIs) and ferromagnesian chondrules. Therefore, the study of aluminum-rich chondrules can provide us with insights on the genetic and temporal relationship among important components of primitive chondrites.

Relatively little is known about aluminum-rich chondrules in unequilibrated enstatite chondrites (UECs). In part, this is because aluminum-rich chondrules are extremely rare in most UECs. Prior to this study, the ^{26}Al - ^{26}Mg system had been examined in only two aluminum-rich chondrules in enstatite chondrites (Grossman et al. 1995), and no oxygen isotopic data have ever been reported for these objects.

Following up on our earlier investigations of the ^{26}Al - ^{26}Mg systematics and oxygen isotopic characteristics of CAIs in UECs (Guan et al. 2000a, 2000b), we present in this paper the results of a correlated study of oxygen isotopes and ^{26}Al - ^{26}Mg systematics of aluminum-rich chondrules in UECs. The motivation for this study is twofold: First, to better understand the relationship of aluminum-rich chondrules to both CAIs and ferromagnesian chondrules in UECs in an analogous way to what has been done in other unequilibrated chondrite types, and to compare them with their cousins in those other chondrite varieties; and, second, to better understand the distribution of ^{26}Al in the enstatite chondrite formation region and to compare that with the observations from other groups of chondrites. Preliminary data from this study were reported previously in two abstracts (Guan et al. 2002, 2004b).

ANALYTICAL TECHNIQUES

The aluminum-rich chondrules were found by making elemental X-ray area maps of entire polished UEC thin sections, using an energy dispersive X-ray detector on a JEOL JSM-840 scanning electron microscope (SEM). The major-element chemistry of minerals was determined with a JEOL-JXA 8900R electron microprobe operated at 15 kV with a probe current of 5–20 nA.

In situ oxygen isotopes of one aluminum-rich chondrule were measured (along with those of UEC CAIs) (Guan et al. 2000b) with the CAMECA IMS 1270 ion microprobe at UCLA; the techniques are described in McKeegan et al. (1998). Oxygen isotope analyses of five more aluminum-rich chondrules were carried out with the CAMECA IMS 6f ion microprobe at Arizona State University (ASU). A detailed description of the analytical approach is given in Jones et al. 2004. Briefly, a 0.2–0.4 nA beam of Cs^+ was focused onto a spot of ~20 μm in diameter in aperture illumination mode. The sample voltage was set to -9 kV and secondary ions were collected by peak-jumping into either a Faraday cup ($^{16}\text{O}^-$) or electron multiplier ($^{17}\text{O}^-$ and $^{18}\text{O}^-$) at a mass resolving power of ~6000, which is sufficient to completely resolve the $^{16}\text{OH}^-$ interference on $^{17}\text{O}^-$. Terrestrial standards (San Carlos olivine and Burma spinel) were used to correct instrumental mass fractionation. Matrix effect under such analytical conditions is mostly correlated with Fe contents of minerals analyzed (Hua et al. 2005). Therefore, even though San Carlos olivine was used to calibrate instrumental mass fractionation for plagioclase or glasses, variations in the matrix effect among these mineral are small (~1–2%). Uncertainties on individual

analyses are ~2–3‰ (2σ), taking into account the variation on repeated analyses of standards and counting statistical errors.

The magnesium isotopic compositions of five aluminum-rich chondrules were first measured with PANURGE, a modified CAMECA IMS 3f ion microprobe at Caltech, using the techniques described in Fahey et al. (1987). Additional data for eight aluminum-rich chondrules were obtained with the ion microprobe at ASU, using procedures similar to those described in MacPherson et al. (2003). Briefly, a ~0.1 nA O^- primary beam was focused onto a <5 μm diameter spot for all the analyses. The sample voltage was set to +9 kV and secondary ions were collected with an energy band-pass of ~45 eV, an imaged field of ~75 m, and a mass resolving power of ~3500. The masses measured were ^{24}Mg , ^{25}Mg , ^{26}Mg , and ^{27}Al . Excesses of ^{26}Mg ($\equiv^{26}\text{Mg}^*$), corrected for both instrumental and intrinsic mass fractionations, were calculated using a linear law; for the high Al/Mg minerals measured in these chondrules, possible errors in determining radiogenic $^{26}\text{Mg}^*$ due to an incorrectly applied mass fractionation correction are insignificant. The Al/Mg sensitivity factors were determined using terrestrial standards including spinel, melilite, and plagioclase.

RESULTS

Thirty polished thin sections of eighteen UECs were examined for this study. Thirteen of the meteorites contain no aluminum-rich chondrules with high Al/Mg mineral phases that are suitable for this study. The remaining three EH3 meteorites (ALHA77295, EET 87746, and Sahara 97072) and two (paired) EL3 meteorites (LEW 87220, LEW 87234) yielded thirteen aluminum-rich chondrules and two plagioclase fragments that were studied in detail for ^{26}Al - ^{26}Mg systematics or oxygen isotopes. Brief descriptions of their petrography and mineralogy are given below.

Petrography and Mineralogy

The thirteen aluminum-rich chondrules and two plagioclase fragments range from ~50 to 420 μm in diameter. The chondrules vary considerably in mineralogy and textures, typical of aluminum-rich chondrules; a summary is given in Table 1. The chondrules are classified according to the phase-equilibrium-based nomenclature of MacPherson and Huss (2005). Briefly, aluminum-rich [Plg] chondrules have textures dominated by long euhedral plagioclase laths and whose bulk compositions are such that plagioclase \rightarrow spinel or spinel \rightarrow plagioclase is the expected liquidus assemblage. Aluminum-rich [Ol] chondrules have olivine (or spinel) as the liquidus phase; in silica-rich varieties, spinel is absent and low-calcium pyroxene (enstatite or pigeonite) may be present. Aluminum-rich [Glass] chondrules are separate: They are characterized by abundant iron- and sodium-rich and calcium-poor glass, and their bulk compositions have

Table 1. Chondrules and fragments analyzed in this study.

Chondrule	E4640-2	L2003-2	L3409-11	S7203-5	A9551-4
Meteorite	EET 87746	LEW 87220	LEW 87234	Sahara 97072	ALHA77295
Al-rich chondrule type ^a	[Plg]	[Plg]	[Plg]	[Plg]	[Plg]
Crystallization sequence ^b	Plg→Diop	Sp→Plg→Diop→En	Plg→Diop→En	Plg→(Diop, En)→glass	Plg→Diop→glass
Plg. comp.	An _{81–98}	An _{66–71}	An _{90–100}	An _{83–94}	An _{70–81}
Chondrule	E4631-7	S7202-17	E4631-4	L2003-1	E4631-5
Meteorite	EET 87746	Sahara 97072	EET 87746	LEW 87220	EET 87746
Al-rich chondrule type	[Ol]	[Ol]	[Glass]	[Ol]	[Glass]
Crystallization sequence	Fo→(En, Plg)→Diop	Fo→(En, Plg)	Diop→glass	(Sp, Fo)→Diop→glass	En→SiO ₂ →Diop→glass
Plg. comp.	An _{65–71}	An _{72–78}	—	—	—
Chondrule	E4642-1	E4642-2	S7202-1	L3409-12	A9528-10
Meteorite	EET 87746	EET 87746	Sahara 97072	LEW 87234	ALHA77295
Al-rich chondrule type	[Glass]	[Glass]	[Glass]	Crystal fragment	Crystal fragment
Crystallization sequence	Sp→Diop→glass	En→Diop→glass	(En, Diop)→glass	—	—
Plg. comp.	—	—	—	An _{80–84}	An ₈₀

^aThe phases listed in brackets are the liquidus (phenocryst) phases. See MacPherson and Huss (2005).

^bPhases are listed in the inferred order of first appearance during melt crystallization. Phases listed together in parentheses means that their relative order is unclear. Metal and sulfide are not included.

Abbreviations: Plg = plagioclase; Diop = diopsidite; Sp = spinel; En = enstatite; Ol = olivine; Fo = forsterite.

anomalously low Ca/Al ratios, which is suggestive of complex processing that included plagioclase alteration accompanied by calcium loss and followed by remelting (MacPherson and Huss 2005).

Based on textures, mineral assemblages, and preliminary major-element analyses, five of these chondrules (A9551-4,¹ E4640-2, L2003-2, L3409-11, and S7203-5) fall into the aluminum-rich [Plg] category. Their textures are dominated by long plagioclase laths (An_{65–93}) with interstitial enstatite and/or aluminous diopsidite, and lesser amounts of spinel, olivine, mesostasis, troilite, and Fe-Ni metal. Mineral chemistry and textures indicate that the plagioclase not only is a primary igneous phase in these aluminum-rich chondrules but also was the liquidus phase. E4640-2 (Fig. 1a) is a small (~100 µm in diameter) subophitic-textured pyroxene-plagioclase chondrule from EET 87746, with the diopsidite containing up to 33 wt% Al₂O₃. L2003-2 (Fig. 1b) is a porphyritic chondrule, ~250 µm in diameter, composed mainly of plagioclase and enstatite, with minor spinel (enclosed in plagioclase) and aluminum-rich diopsidite. L3409-11 (Fig. 1c) is a relatively large (~320 µm) chondrule whose texture is dominated by long plagioclase laths, interstitial to which are subordinate enstatite and diopsidite.

¹ Aluminum-rich chondrules are labeled with a shorthand notation as follows: the first three characters represent the first letter and last two numbers from the meteorite name, the next two digits are the individual thin section number, and the last digit is the specific chondrule identification number; e.g., A9551-4 is aluminum-rich chondrule #4 from ALH 77295 PTS#51, and E4631-4 is aluminum-rich chondrule #4 from EET 87746 PTS#31.

S7203-5 (Fig. 1d) is an oval-shaped chondrule, ~200 × 100 µm in size, whose texture also is dominated by long plagioclase laths; enstatite, aluminous diopsidite, and glassy material are interstitial. A9551-4 (Fig. 1e) is a broken fragment, ~130 µm in maximum dimension, of what is probably a compound object. One part is an aluminum-rich [Plg] chondrule, consisting of euhedral plagioclase laths and minor interstitial diopsidite and sodium-rich glass. The other part is nearly monomineralic enstatite.

Three of the chondrules are aluminum-rich [Ol] chondrules. E4631-7 (Fig. 1f) is a ~210 µm chondrule fragment whose texture is dominated by large (30–50 µm) enstatite crystals that in places enclose smaller olivine crystals, and a fine interstitial intergrowth of plagioclase (An_{60–71}) and diopsidite. S7202-17 (Fig. 1g) is ~150 µm in diameter and has a concentrically zoned structure. The mantle consists of large enstatite crystals enclosing rounded olivine crystals. The chondrule interior contains intergrown plagioclase (An_{67–85}), olivine, and troilite. Chondrule L2003-1 is ~420 µm in size and contains a few crystals of spinel, skeletal olivine, and rare enstatite enclosed in a very fine-grained mesostasis of glass and dendritic aluminous diopsidite (Fig. 1h).

E4631-4 and S7202-1 are aluminum-rich [Glass] chondrules. S7202-1 is mostly sodium-rich and calcium-poor glass with a few small crystals of enstatite and diopsidite. E4631-4 (Fig. 1i) consists of long spongy blades of pyroxene (diopsidite rims enclosing low-calcium pyroxene cores) in a sodium-rich and calcium-poor glass matrix.

E4642-2 and E4631-5 are not easily classified. E4642-2

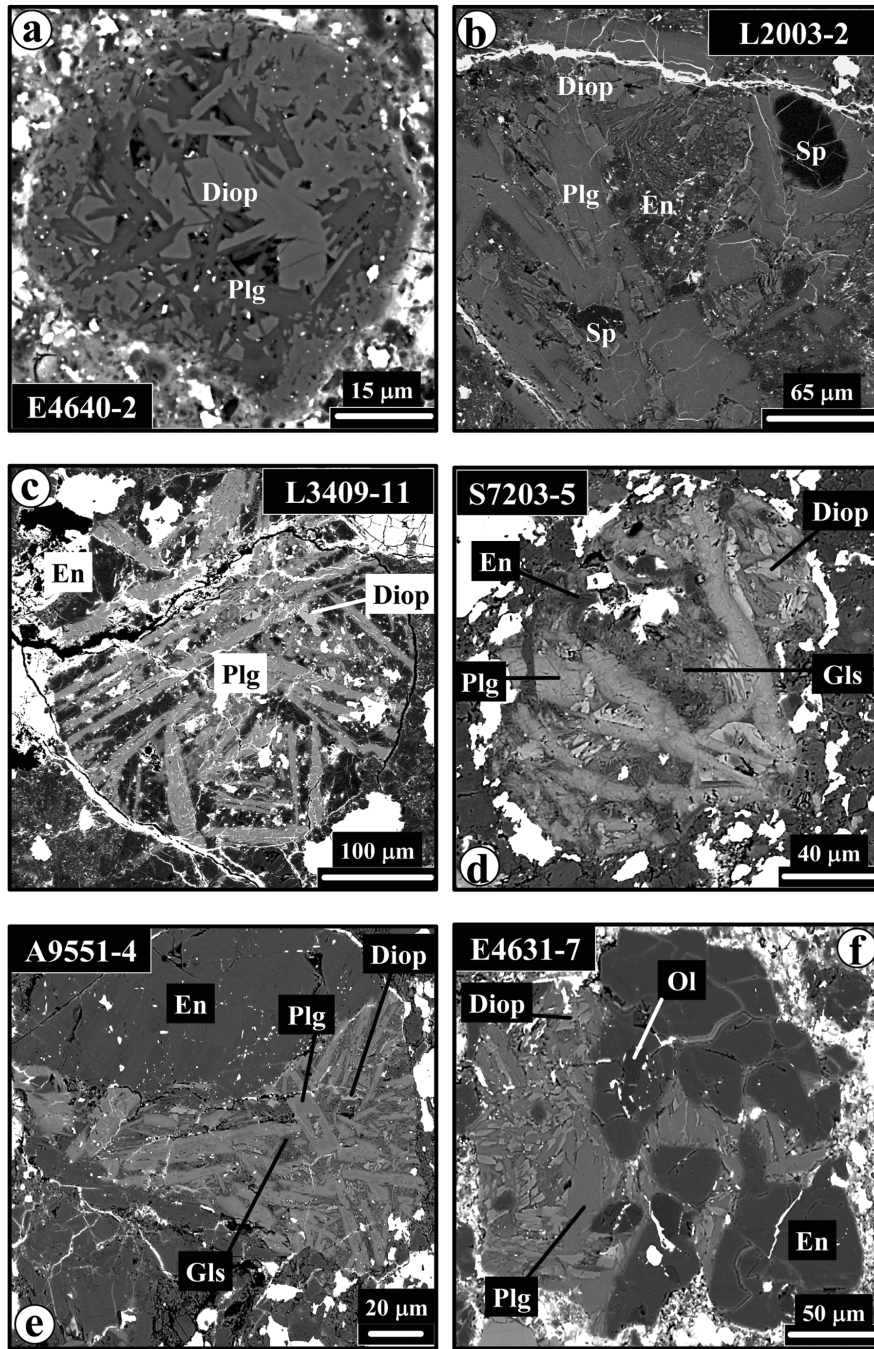


Fig. 1. Backscattered electron images of aluminum-rich chondrules from unequilibrated enstatite chondrites. Sp = spinel; Plg = plagioclase; Diop = diopside; Gls = glass; En = enstatite; Ol = olivine; FeS = troilite; I.P. = ion microprobe crater.

appears to be a chondrule fragment consisting of blocky enstatite and diopside crystals sitting in a matrix of tiny skeletal diopside crystallites and sodium-rich glass. E4631-5 (~170 μm in diameter) (Fig. 1j) has a mantle of pure crystalline SiO_2 enclosing an interior that consists of sparse blocky enstatite grains and one large troilite inclusion embedded in a fine-grained mesostasis of potassium-rich, sodium-poor glass and dendritic diopside crystals.

Two isolated plagioclase fragments were studied. L3409-12 (Fig. 1k) is a ~250 μm size triangular plagioclase (An_{90-100}) fragment in LEW 87234. A9528-10 (An_{80}) is ~85 μm in its largest dimension. Both contain terrestrial iron oxide veins crisscrossing through their boundaries, and a small portion of A9528-10 has been replaced by Na-rich plagioclase (An_3).

Chondrule E4642-1 (Fig. 1l) was previously described

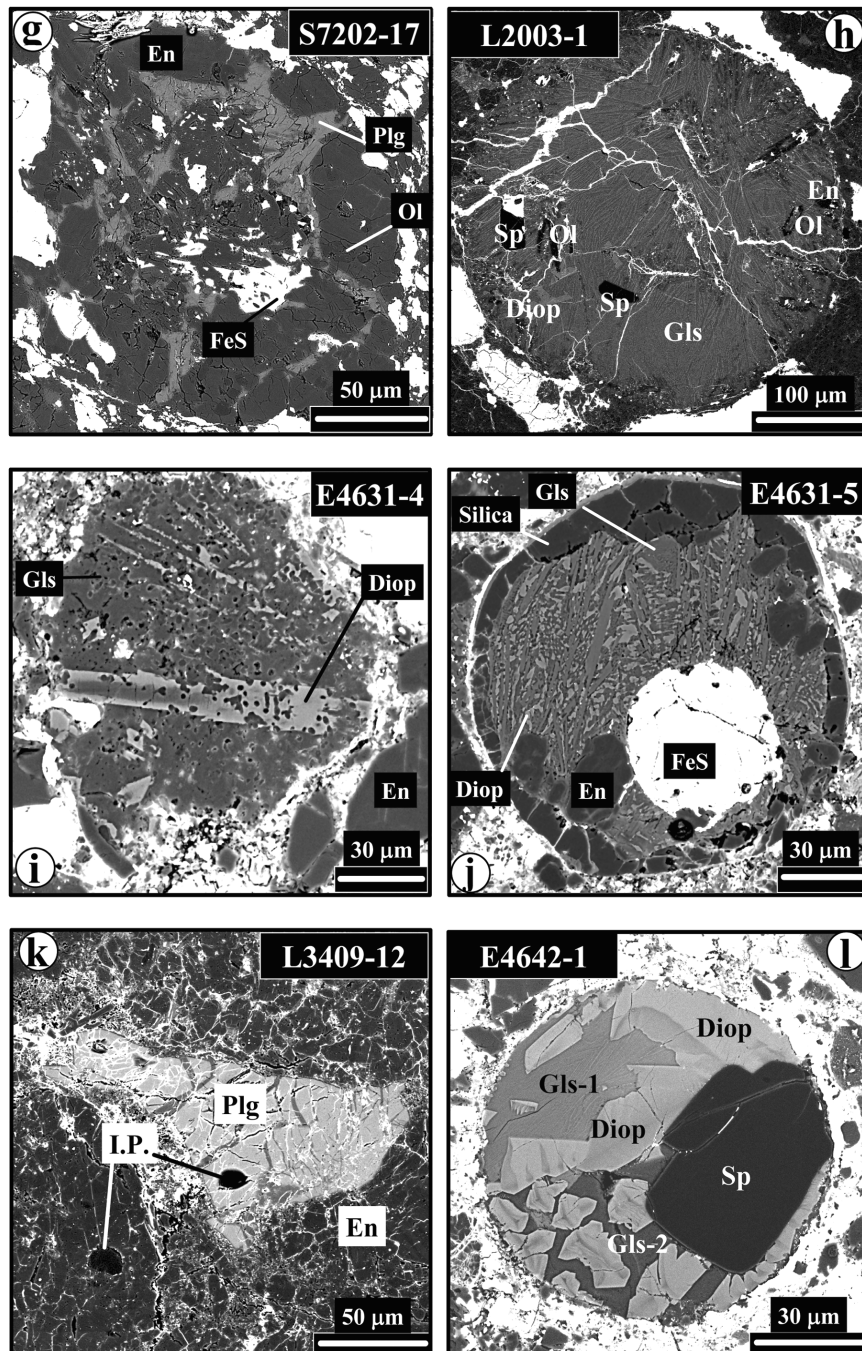


Fig. 1. *Continued.* Backscattered electron images of aluminum-rich chondrules from unequilibrated enstatite chondrites. Sp = spinel; Plg = plagioclase; Diop = diopside; Gls = glass; En = enstatite; OI = olivine; FeS = troilite; I.P. = ion microprobe crater.

by Guan et al. (2000b). Briefly, this almost-perfectly spherical chondrule (~100 μm in diameter) consists of large blocky spinel (up to $\sim 20 \times 50 \mu\text{m}$) partially enclosed by quench-textured aluminous diopside and two types of glass ($\text{CaO} \sim 9\text{--}12\%$, $\text{Na}_2\text{O} \sim 3\text{--}4\%$; and $\text{CaO} < 2\%$, $\text{Na}_2\text{O} \sim 10\text{--}11\%$).

Al-Mg Isotopic Systematics

Eleven of the aluminum-rich chondrules and the two

plagioclase crystal fragments were analyzed for magnesium isotopes. The results are listed in Table 2, and data for six chondrules are plotted in Fig. 2.

Of the thirteen aluminum-rich objects analyzed, only one aluminum-rich chondrule (S7203-5) has clearly resolved excesses of ^{26}Mg that correlate with $^{27}\text{Al}/^{24}\text{Mg}$ (Table 2; Fig. 2a). The inferred $(^{26}\text{Al}/^{27}\text{Al})_0$ is $(0.68 \pm 0.24) \times 10^{-5}$, significantly lower than the “canonical” value ($\sim 5 \times 10^{-5}$) found in most CAIs.

Table 2. Magnesium isotopic data for aluminum-rich chondrites from UECs.

Al chondrules	$(^{27}\text{Al}/^{26}\text{Mg}) \pm 2\sigma$	$\delta^{26}\text{Mg}^* \pm 2\sigma^a$	$(^{26}\text{Al}/^{27}\text{Mg})_0 \pm 2\sigma$
A9528-10			$(0.03 \pm 2.4) \times 10^{-5}$
En#1	0.030 ± 0.003	0.1 ± 0.2	
Plg#1	29.2 ± 1.1	1.3 ± 5.5	
Plg#2	14.5 ± 2.5	-4.9 ± 9.9	
Plg#3	21.5 ± 2.2	-2.5 ± 13.5	
A9551-4			$(-1.5 \pm 5.2) \times 10^{-6}$
En#1	0.005 ± 0.0005	0.5 ± 1.9	
En#2	0.013 ± 0.001	-0.9 ± 2.0	
Gls#1	6.43 ± 0.04	-2.4 ± 2.7	
Plg#1a	61.4 ± 1.2	-1.6 ± 9.5	
Plg#1b	72.3 ± 4.3	8.3 ± 11.6	
Plg#2a	217.2 ± 6.6	4.4 ± 13.7	
Plg#2b	164.3 ± 7.0	-6.9 ± 8.0	
E4631-4			$(1.3 \pm 2.4) \times 10^{-6}$
En#1	0.020 ± 0.002	0.8 ± 1.9	
En#2	0.074 ± 0.002	-0.3 ± 0.9	
En#3	0.024 ± 0.001	0.1 ± 2.6	
Plg#1	220.3 ± 8.3	2.8 ± 10.2	
Plg#2	288 ± 11	6.6 ± 10.4	
Plg#3	390 ± 21	0.9 ± 11.4	
Plg#4	309 ± 11	1.2 ± 10.1	
E4631-5			$(1.1 \pm 2.6) \times 10^{-5}$
Gls#1a	21.9 ± 1.2	13.1 ± 12.9	
Gls#1b	12.7 ± 0.8	-2.7 ± 7.9	
Gls#2a	26.8 ± 1.4	3.5 ± 9.8	
Gls#2b	23.9 ± 1.4	1.9 ± 9.6	
Gls#3	36.0 ± 1.8	-2.1 ± 11.6	
E4631-7			$(1.6 \pm 2.3) \times 10^{-5}$
Plg#1a	15.9 ± 1.6	5.7 ± 5.7	
Plg#1b	14.6 ± 1.5	-1.0 ± 8.4	
Plg#2a	13.6 ± 1.4	3.4 ± 7.0	
Plg#2b	15.2 ± 1.5	1.8 ± 4.6	
Plg#2c	18.0 ± 1.8	-0.7 ± 4.9	
E4640-2			$(0.74 \pm 4.2) \times 10^{-5}$
Diop#1	0.34 ± 0.03	1.2 ± 3.0	
Plg#1	16.3 ± 1.6	-2.7 ± 8.7	
Plg#2	18.4 ± 1.8	5.4 ± 6.8	
Plg#3	18.1 ± 1.8	1.3 ± 7.2	
E4642-2			$(-0.39 \pm 1.2) \times 10^{-5}$
Diop#1	0.51 ± 0.02	-0.1 ± 2.0	
Diop#2	1.97 ± 0.10	-0.6 ± 4.3	
Gls#1a	7.08 ± 0.43	-2.0 ± 6.0	
Gls#1b	9.03 ± 0.46	-1.1 ± 4.1	
Gls#2a	16.9 ± 0.9	2.4 ± 6.9	
Gls#2b	13.9 ± 1.0	-2.3 ± 4.7	
Gls#2c	12.3 ± 0.6	-1.6 ± 2.8	
Gls#3a	70.1 ± 6.0	2.3 ± 10.9	
Gls#3b	37.8 ± 1.9	-2.5 ± 5.3	
Gls#3c	27.9 ± 2.4	7.1 ± 11.0	
L2003-2			$(0.0 \pm 1.1) \times 10^{-6}$
Sp#1	2.32 ± 0.12	-2.1 ± 2.1	
Sp#2	2.23 ± 0.12	0.0 ± 2.2	
Sp#3	2.23 ± 0.12	-0.1 ± 3.5	
Sp#4	2.22 ± 0.12	0.0 ± 2.1	

Table 2. *Continued.* Magnesium isotopic data for aluminum-rich chondrites from UECs.

Al chondrules	$(^{27}\text{Al}/^{26}\text{Mg}) \pm 2\sigma$	$\delta^{26}\text{Mg}^* \pm 2\sigma^a$	$(^{26}\text{Al}/^{27}\text{Mg})_o \pm 2\sigma$
Sp#5	2.22 ± 0.12	-0.3 ± 2.1	
Sp#6	2.24 ± 0.12	0.6 ± 2.0	
Sp#7	2.22 ± 0.12	0.7 ± 1.9	
An#1a	111.2 ± 7.2	2.8 ± 6.9	
An#1b	159.1 ± 8.6	0.5 ± 7.7	
An#2a	1305 ± 75	-7 ± 20	
An#2b	1051 ± 67	1 ± 17	
An#3a	968 ± 57	4 ± 19	
An#3b	718 ± 39	1 ± 13	
An#3c	426 ± 31	-1 ± 11	
L3409-12			$(-0.3 \pm 0.6) \times 10^{-6}$
En#1	0.0160 ± 0.0009	0.2 ± 2.0	
En#2	0.0160 ± 0.0009	0.1 ± 2.0	
En#3	0.0164 ± 0.0009	-0.4 ± 0.2	
Plg#1a	738 ± 42	9 ± 17	
Plg#1b	531 ± 51	-5 ± 22	
Plg#2a	1130 ± 61	4 ± 15	
Plg#2b	1900 ± 102	-1 ± 19	
Plg#2c	1596 ± 88	1 ± 19	
Plg#3a	2038 ± 109	-12 ± 22	
Plg#3b	2249 ± 120	-17 ± 20	
L3409-11			$(0.15 \pm 1.4) \times 10^{-5}$
En#1	0.0160 ± 0.0009	0.1 ± 2.0	
En#2	0.0164 ± 0.0009	-0.4 ± 0.2	
En#3	0.0160 ± 0.0009	0.2 ± 2.0	
(Plg,En)#1	16.25 ± 0.91	-0.2 ± 1.8	
(Plg,En)#2	17.12 ± 0.93	-0.3 ± 3.6	
S7202-1			$(-0.7 \pm 9.5) \times 10^{-6}$
En#1	0.030 ± 0.003	0.1 ± 0.2	
Gls#1	67.9 ± 4.9	3.2 ± 8.7	
Gls#2	118.4 ± 5.0	-1.6 ± 9.8	
Gls#3	37.1 ± 5.2	-7.8 ± 12.2	
Gls#4	19.5 ± 2.0	-1.2 ± 12.7	
S7202-17			$(0.2 \pm 9.2) \times 10^{-6}$
Plg#1	30.5 ± 1.1	0.0 ± 4.5	
Plg#2	29.5 ± 1.1	0.5 ± 6.5	
Plg#3	34.4 ± 1.7	2.5 ± 7.6	
Plg#4	73.8 ± 7.7	-0.4 ± 6.2	
S7203-5			$(6.8 \pm 2.4) \times 10^{-6}$
En#1	0.32 ± 0.02	2.7 ± 3.8	
En#2	1.69 ± 0.10	3.1 ± 6.4	
Gls#1a	19.3 ± 2.0	2.0 ± 8.7	
Gls#1b	15.2 ± 0.9	-0.4 ± 5.6	
Gls#1c	12.3 ± 0.7	-3.2 ± 5.3	
Plg#1a	27.4 ± 2.1	-5.4 ± 7.7	
Plg#1b	26.0 ± 5.4	-6.4 ± 11.5	
Plg#2a	77.5 ± 6.2	6.1 ± 10.0	
Plg#2b	52.6 ± 3.1	6.4 ± 8.5	
Plg#2c	55.8 ± 3.2	0.5 ± 9.0	
Plg#3a	699 ± 41	36 ± 20	
Plg#3b	738 ± 44	29 ± 19	
Plg#4a	369 ± 14	17 ± 19	
Plg#4b	271.7 ± 8.0	23 ± 14	
Plg#4c	164.6 ± 6.9	17 ± 14	
Plg#4d	110.6 ± 5.9	1.5 ± 8.1	

^a $\delta^{26}\text{Mg}^*$ is related to $^{26}\text{Mg}/^{24}\text{Mg}$ by: $\delta^{26}\text{Mg}^* = ((^{26}\text{Mg}/^{24}\text{Mg}_{\text{meas}})/0.13932) - 1) \times 1000$.

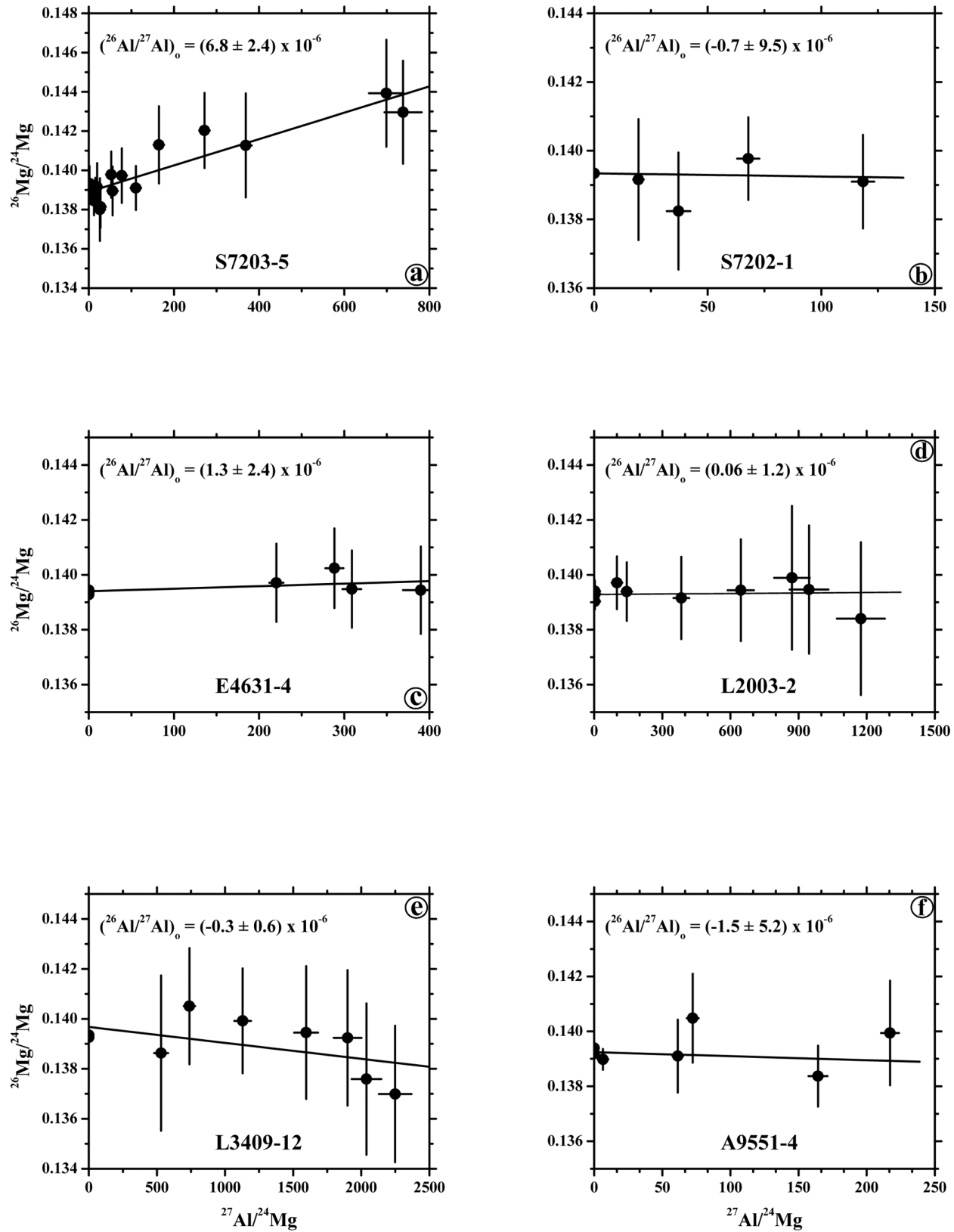


Fig. 2. ^{26}Al - ^{26}Mg systematics of aluminum-rich chondrules from unequilibrated enstatite chondrites.

Table 3. Oxygen isotopic composition of aluminum-rich chondrules from UECs.

Spot analysis	$\delta^{18}\text{O} (\pm 2\sigma)^{\text{a}}$ (‰)	$\delta^{17}\text{O} (\pm 2\sigma)$ (‰)	$\Delta^{17}\text{O}^{\text{b}}$ ($\pm 2\sigma$) (‰)
E4642-1Sp1	-2.7 ± 2.9	-3.5 ± 1.8	-2.1 ± 2.4
E4642-1Sp2	-1.1 ± 2.8	-1.9 ± 2.4	-1.3 ± 2.8
E4642-1Diop	0.9 ± 2.8	-1.9 ± 2.0	-2.4 ± 2.5
E4642-1Gls	-2.3 ± 2.7	-2.1 ± 2.3	-0.9 ± 2.6
E4640-2Diop1	6.0 ± 3.3	2.0 ± 2.3	-1.2 ± 2.8
E4640-2Gls1	6.7 ± 3.3	3.9 ± 2.3	0.4 ± 2.8
L2003-2Sp1	-2.8 ± 3.3	-4.8 ± 2.4	-3.4 ± 3.0
L2003-2Sp2	-1.0 ± 3.2	-1.7 ± 2.1	-1.2 ± 2.6
L2003-2Sp3	0.1 ± 3.3	-2.9 ± 2.1	-2.9 ± 2.7
L2003-2Plg1	3.1 ± 3.3	0.7 ± 2.3	-0.9 ± 2.9
L2003-2Plg2	5.8 ± 3.2	2.2 ± 2.2	-0.8 ± 2.8
L2003-1Sp1	-0.1 ± 3.4	-0.9 ± 2.4	-0.9 ± 3.0
L2003-1Sp2	2.6 ± 3.2	-0.4 ± 2.3	-1.7 ± 2.8
L2003-1Sp3	3.6 ± 3.2	-0.6 ± 2.2	-2.5 ± 2.7
L2003-1Ol1	-0.3 ± 3.3	-1.2 ± 2.3	-1.0 ± 2.9
L2003-1Ol2	1.3 ± 3.2	-1.0 ± 2.2	-1.7 ± 2.8
L2003-1(Gls + Diop)	4.6 ± 3.3	1.7 ± 2.1	-0.7 ± 2.7
L2003-1Gls1	5.3 ± 3.5	1.8 ± 2.2	-1.0 ± 2.8
L2003-1Gls2	4.2 ± 3.3	1.5 ± 2.3	-0.7 ± 2.9
L3409-12Plg	1.1 ± 2.0	-0.7 ± 1.9	-1.2 ± 2.2
S7203-5Diop1	-4.1 ± 2.0	-2.9 ± 2.0	-0.7 ± 2.2
S7203-5(Diop + Gls)	-5.3 ± 2.1	-3.6 ± 1.9	-0.9 ± 2.2
S7203-5Gls	-1.1 ± 2.0	-1.1 ± 2.0	-0.5 ± 2.3
S7203-5(Plg + Diop)	-1.5 ± 2.0	-1.3 ± 2.0	-0.6 ± 2.2
S7203-5(Plg + Diop)	-0.7 ± 3.0	-0.3 ± 2.5	0.1 ± 2.9
S7203-En	-0.8 ± 2.1	-0.5 ± 1.9	-0.1 ± 2.2
L3409-En	-1.7 ± 2.0	-1.0 ± 2.0	-0.1 ± 2.2

^aOxygen isotopic compositions are expressed as δ -values, the deviation in per mil relative to a standard composition (standard mean ocean water: SMOW): $\delta^{\text{m}}\text{O} = [({}^{\text{m}}\text{O}/{}^{16}\text{O})_{\text{sample}} / (({}^{\text{m}}\text{O}/{}^{16}\text{O})_{\text{SMOW}} - 1)] \times 1000$, where $m = 17$ or 18.

^bThe deviation of the oxygen isotopic composition from the terrestrial fractionation line is expressed by $\Delta^{17}\text{O}$, where $\Delta^{17}\text{O} = \delta^{17}\text{O} - 0.52\delta^{18}\text{O}$.

Abbreviations: Sp = spinel; Diop = diopside; Gls = glass; Plg = plagioclase; Ol = olivine; En = enstatite.

None of the other aluminum-rich chondrules or the plagioclase grains display resolved ${}^{26}\text{Mg}^*$ (Figs. 2b–2f). The Al/Mg ratios in some of them (e.g., A9528-10, E4631-5, and E4631-7) are low, and within the relatively large errors there are no detectable ${}^{26}\text{Mg}$ excesses; the $({}^{26}\text{Al}/{}^{27}\text{Al})_0$ ratios are consistent with zero. Although the large errors in some aluminum-rich chondrules (e.g., S7202-1 and S7202-17) result in upper limits on the $({}^{26}\text{Al}/{}^{27}\text{Al})_0$ ratios similar to that inferred for S7203-5, the best constrained upper limit (with the smallest error) of the inferred $({}^{26}\text{Al}/{}^{27}\text{Al})_0$ values is probably $\sim 1 \times 10^{-6}$, determined from the aluminum-rich chondrules with the highest Al/Mg ratios (e.g., L2003-2, L3409-12, and A9551-4).

Oxygen Isotopes

Oxygen isotope compositions were measured in five aluminum-rich chondrules and one plagioclase fragment. For comparison, two enstatite grains in ferromagnesian

chondrules from LEW 87234 and Sahara 97072 were also analyzed for their oxygen isotopes. The results are listed in Table 3 and are plotted in Figs. 3 and 4. Shown in the figures also for reference are the oxygen isotopic compositions of bulk ferromagnesian chondrules and whole rock of enstatite chondrites (Clayton et al. 1984; Clayton and Mayeda 1985).

On a three-isotope diagram (Fig. 3a), the oxygen isotopic compositions of the five UEC aluminum-rich chondrules and a plagioclase fragment overlap those of UEC ferromagnesian chondrules at the ${}^{16}\text{O}$ -poor end, but extend to more ${}^{16}\text{O}$ -rich compositions; the overall spread (expressed in terms of $\delta^{18}\text{O}$) is $\sim 12\text{‰}$. Because of the large scatter of the data points and the size of the analytical errors, the combined oxygen isotope data for the aluminum-rich chondrules only roughly determine a correlation line having slope 0.6 ± 0.1 . This line is not resolvable from the lines defined by bulk ferromagnesian chondrules (slope = 0.7 ± 0.1) (Clayton and Mayeda 1985) or by bulk enstatite chondrites (slope ~ 0.5) (Clayton et al. 1984; Newton et al. 2000).

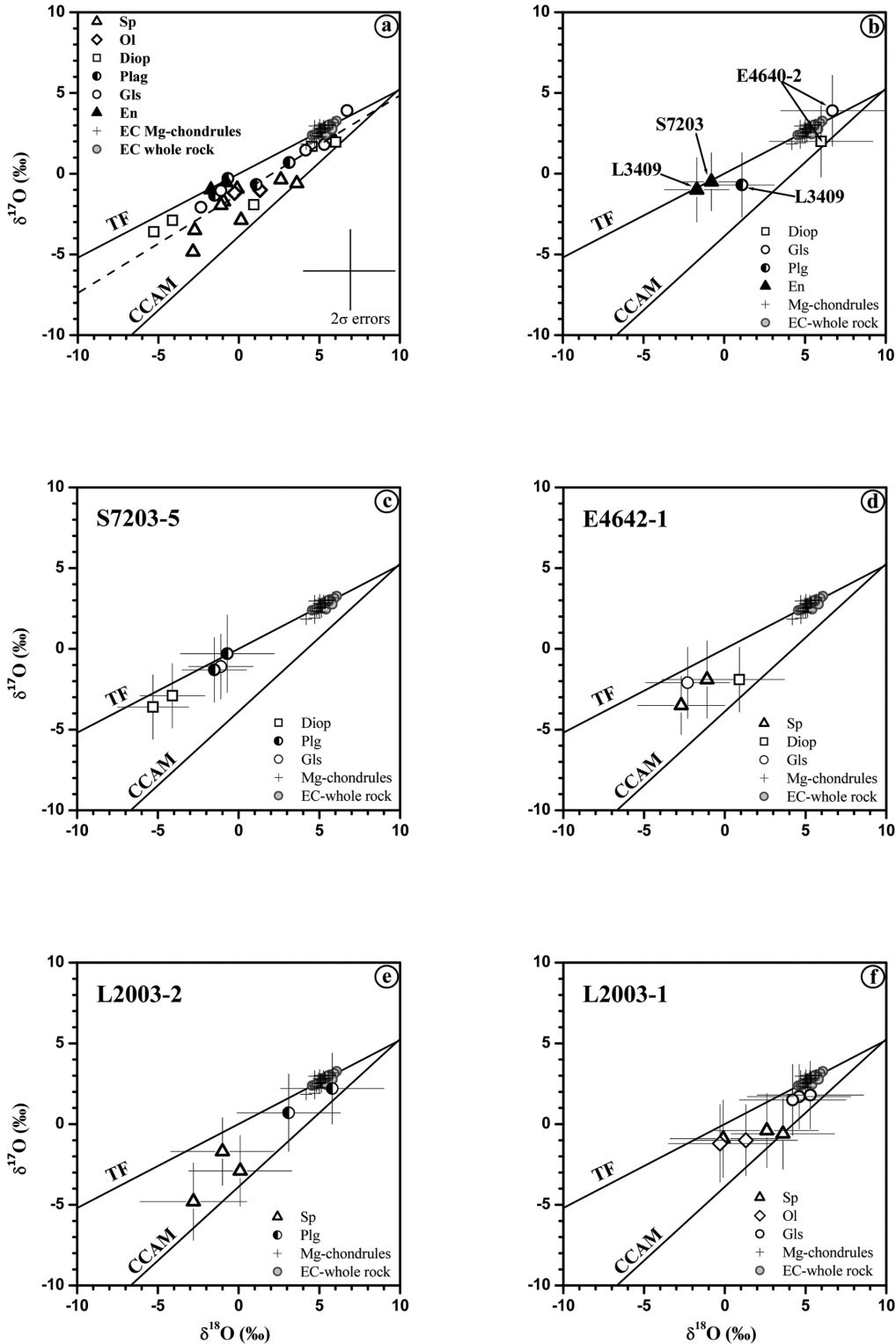


Fig. 3. The oxygen isotope compositions of aluminum-rich chondrules from unequilibrated enstatite chondrites. a) All the oxygen isotopic data of the five aluminum-rich chondrules and a plagioclase fragment roughly define a regression line (dashed) with a slope of 0.6 ± 0.1 . b–f) The oxygen isotope compositions of individual chondrules or minerals. The high-precision bulk data for EC whole rock and Mg-rich chondrules are from Clayton et al. (1976, 1984) and Clayton and Mayeda (1985). TF = terrestrial fractionation line; CCAM = carbonaceous chondrite anhydrous minerals; Sp = spinel; Diop = diopside; Plag = plagioclase; Gls = glass; Ol = olivine; En = enstatite from ferromagnesian chondrules.

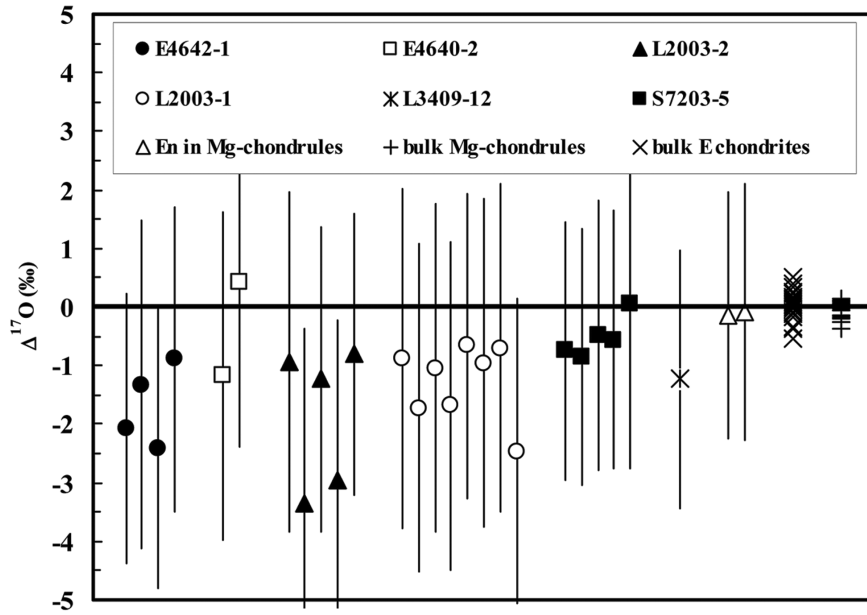


Fig. 4. The deviations from the terrestrial fractionation line of aluminum-rich chondrules in unequilibrated enstatite chondrites. $\Delta^{17}\text{O} = \delta^{17}\text{O} - 0.52 \times \delta^{18}\text{O}$. High-precision bulk data for EC whole rock and Mg-rich chondrules are shown for comparison (data sources: Clayton et al. 1976, 1984; Clayton and Mayeda 1985).

The most ^{16}O -poor chondrule is E4640-2, which falls within the ranges of UEC ferromagnesian chondrules and bulk enstatite chondrites (Clayton and Mayeda 1985; Newton et al. 2000; Okazaki and Huss 2003) (Fig. 3b). The other four aluminum-rich chondrules and the plagioclase fragment are more ^{16}O -enriched, plotting along an extension of the line defined by the ferromagnesian chondrules (Figs. 3b–3f). S7203-5 and E4642-1 are the most ^{16}O -enriched, with ^{18}O down to $\sim -5\text{\textperthousand}$ and $\delta^{17}\text{O}$ to $\sim -4\text{\textperthousand}$. Surprisingly, the two enstatite grains (S7203-En and L3409-En) from ferromagnesian chondrules fall on the terrestrial fractionation (TF) line at much lower $\delta^{18}\text{O}$ values than UEC ferromagnesian chondrules and bulk enstatite chondrites; they overlap with the data for one of the aluminum-rich chondrules (S7203-5) (Figs. 3b–c). The spread in $\delta^{18}\text{O}$ and $\delta^{17}\text{O}$ values along a mass fractionation line for an individual chondrule shown in Fig. 3 might be attributed to instrumental mass fractionation or matrix effect. Probably due to the same causes, there is not a completely uniform pattern to the isotopic heterogeneity among different mineral phases in aluminum-rich chondrules. Spinel and diopside are the most ^{18}O -depleted in some chondrules (e.g., S7203-5, E4642-1, and L2003-2). Plagioclase and glass are generally ^{18}O -rich. In Fig. 4, which shows deviations from the TF line, most data points for the five aluminum-rich chondrules and the plagioclase fragment overlap with the TF line within the errors. The slight ^{16}O -enrichments observed in the aluminum-rich chondrules L2003-2 and E4642-1 indicate that precursor ^{16}O -rich material might have survived melting and isotopic exchange in these chondrules.

DISCUSSION

^{26}Al Distribution in Aluminum-Rich Chondrules of Different Chondrite Groups

Prior to this study, no unambiguous evidence of extinct ^{26}Al had been detected in either ferromagnesian or aluminum-rich chondrules from enstatite chondrites (cf. Grossman et al. 1995). Our detection of $^{26}\text{Mg}^*$ in the aluminum-rich chondrule S7203-5, with $(^{26}\text{Al}/^{27}\text{Al})_0 = (0.68 \pm 0.24) \times 10^{-5}$ means that initial ratios of $(\sim 0.5\text{--}1) \times 10^{-5}$ have now been observed in chondrules from all major chondrite groups (e.g., Russell et al. 1996; Kita et al. 2000; Huss et al. 2001). These chondrule ratios are consistently $5\times\text{--}10\times$ lower than those of most CAIs from the same chondrite groups, which generally are at a level of $(^{26}\text{Al}/^{27}\text{Al})_0 \sim 5 \times 10^{-5}$ (MacPherson et al. 1995; Russell et al. 1996; Guan et al. 2000a; Huss et al. 2001) or even higher (Young et al. 2005).

S7203-5 is the only one out of fifteen aluminum-rich chondrules analyzed from UECs (this study; Grossman et al. 1995) that shows resolvable $^{26}\text{Mg}^*$ consistent with the levels observed in ordinary and carbonaceous chondrite chondrules. In fact, other UEC chondrules with even higher Al/Mg ratios than S7203-5 give upper limits of $(^{26}\text{Al}/^{27}\text{Al})_0 \sim 1 \times 10^{-6}$. It is not clear if this apparent paucity represents a real difference between UEC chondrules and their ordinary and carbonaceous chondrite cousins; the number of analyzed objects from UECs is still too low. And unlike the case for ordinary and carbonaceous chondrites, not enough is understood in detail about enstatite metamorphism

to attribute low initial isotopic ratios to metamorphic effects as opposed to potential isotopic heterogeneities.

For ordinary chondrites, essentially all chondrules from the least metamorphosed LL3.0–3.1 chondrites that have been measured either have initial $(^{26}\text{Al}/^{27}\text{Al})_0$ ratios near 1×10^{-5} or give upper limits consistent with that value (Kita et al. 2000; Huss et al. 2001). These meteorites have never experienced metamorphic temperatures high enough to mobilize Mg (Huss and Lewis 1994; LaTourrette and Wasserburg 1998) or Cr in olivine (Grossman 2004). The loss of Cr in olivine increases dramatically from petrologic types 3.0 and 3.2 for UOCs and can be used as a sensitive indicator of metamorphism and classification (Grossman 2004). In Chainpur (LL3.4), which clearly has been metamorphosed, only about one third of the aluminum-rich chondrules measured contain ^{26}Mg excesses from the in situ decay of ^{26}Al (Russell et al. 1996), with inferred initial $(^{26}\text{Al}/^{27}\text{Al})_0$ ratios ranging from $\sim 5 \times 10^{-6}$ to $\sim 1 \times 10^{-5}$. Ordinary chondrites of higher metamorphic grade, which apparently experienced temperatures high enough to mobilize Mg (Huss and Lewis 1994; LaTourrette and Wasserburg 1998), typically give either no evidence of ^{26}Al or very low initial ratios (Kita et al. 2000; Huss et al. 2001). This relationship suggests that initial ratios of $(\sim 0.5\text{--}1) \times 10^{-5}$ in chondrules from the types 3.0–3.1 ordinary chondrites have not been altered by metamorphism and closely reflect the original ratios at the time of chondrule solidification from an approximately homogeneous isotopic reservoir.

The case is more difficult to quantify for chondrules from carbonaceous chondrites because inferred thermal histories are more complex. Sheng et al. (1991) observed radiogenic $^{26}\text{Mg}^*$ from in situ decay of ^{26}Al in two of the seven aluminum-rich chondrules analyzed in CV chondrites, with inferred $(^{26}\text{Al}/^{27}\text{Al})_0$ ratios at $\sim 3 \times 10^{-6}$ and $\sim 6 \times 10^{-6}$, respectively. Two of four aluminum-rich chondrules from Axtell (CV3) gave initial ratios of $\sim 1 \times 10^{-6}$ and $\sim 3 \times 10^{-6}$ (Srinivasan et al. 2000). Marhas et al. (2000) found that ten out of twenty-two analyzed aluminum-rich chondrules from CV and CR chondrites contained ^{26}Mg excesses, indicating $(^{26}\text{Al}/^{27}\text{Al})_0$ ratios of $(\sim 0.3\text{--}1) \times 10^{-5}$. But most of the objects measured come from meteorites that have experienced more-severe metamorphism than type 3.0–3.1 UOCs (Huss et al., Forthcoming).

Kunihiro et al. (2004) attempted to quantify $(^{26}\text{Al}/^{27}\text{Al})_0$ nebular values during the epoch of chondrule formation by examining ferromagnesian chondrules in one of the most primitive and unaltered carbonaceous chondrites, CO3.0 Yamato 81020. Five FeO-rich chondrules exhibited $^{26}\text{Mg}^*$ in aluminum-rich mesostasis corresponding to $(^{26}\text{Al}/^{27}\text{Al})_0$ within the range $\sim(2\text{--}7) \times 10^{-6}$. Kunihiro et al. (2004) further argued that the mean value observed in chondrules from Yamato 81020, $(^{26}\text{Al}/^{27}\text{Al})_0 = (3.8 \pm 0.7) \times 10^{-6}$, is significantly lower than that found for highly unequilibrated ordinary chondrite chondrules.

Bizzarro et al. (2004) measured whole-chondrules with high-precision ICPMS techniques and inferred very high $(^{26}\text{Al}/^{27}\text{Al})_0$ ratios ($1.36\text{--}5.66 \times 10^{-5}$) for chondrules in Allende. They suggested that the formation of Allende chondrules began contemporaneously with the formation of CAIs. However, because the whole-chondrule data do not provide an internal isochron, these inferred ratios apply to the time of bulk Al-Mg fractionation, possibly during the condensation of chondrule precursor dust grains, and do not constrain the time of last melting of the measured chondrules.

There is little question that type 3 enstatite chondrites have experienced some level of metamorphism. Rubin et al. (1997) observed that all EH3 and EL3 chondrites show evidence of shock metamorphism, and studies of presolar diamonds indicate that UECs could have been heated to as high as 500–600 °C on their parent bodies (Huss and Lewis 1990, 1994). The ^{53}Mn - ^{53}Cr and ^{60}Fe - ^{60}Ni systems in sulfides from UECs have also been more severely disturbed than they have in ordinary chondrites (Guan et al. 2004a; Tachibana and Huss 2003; Mostefaoui et al. 2005). However, no metamorphic subtypes analogous to those for UOCs have been established for enstatite chondrites that would allow placing the range of magnesium isotopic data among different UEC meteorites in a metamorphic context. The most that can be said is that the inferred initial $^{26}\text{Al}/^{27}\text{Al}$ ratio in S7203-5 ($\sim 0.7 \times 10^{-5}$), being consistent with the ratios found in chondrules from the most unequilibrated ordinary and carbonaceous chondrites, further supports the idea that ^{26}Al was widely and at least approximately homogeneously distributed across the chondrite-forming region. If it is assumed that the solar nebula was an initially homogeneous reservoir with $(^{26}\text{Al}/^{27}\text{Al})_0 \sim 5 \times 10^{-5}$, then the lower $(^{26}\text{Al}/^{27}\text{Al})_0$ ratio found in S7203-5 indicates that it formed about 2 My later after the formation of most CAIs.

Oxygen Isotopes of CAIs, Aluminum-Rich Chondrules, and Ferromagnesian Chondrules from UECs

The origin of aluminum-rich chondrules relative to that of normal ferromagnesian ones remains an important unanswered question. Some recent studies have suggested that aluminum-rich chondrules are hybrids, arising from mixing of ferromagnesian chondrule melts with CAI fragments and partial to complete dissolution of the latter (Sheng et al. 1991; Krot and Keil 2002; Krot et al. 2004). In contrast, Russell et al. (2000) argued on the basis of oxygen isotope data that aluminum-rich chondrules from UOCs are not hybrid mixtures of UOC CAIs and ferromagnesian chondrules, but rather are closely related to ferromagnesian chondrules. MacPherson and Huss (2005) used major, minor, and trace-element compositions of aluminum-rich chondrules from UOCs to show that although some aluminum-rich chondrules are consistent with an origin by melting of CAI-ferromagnesian chondrule hybrids, others cannot be so explained.

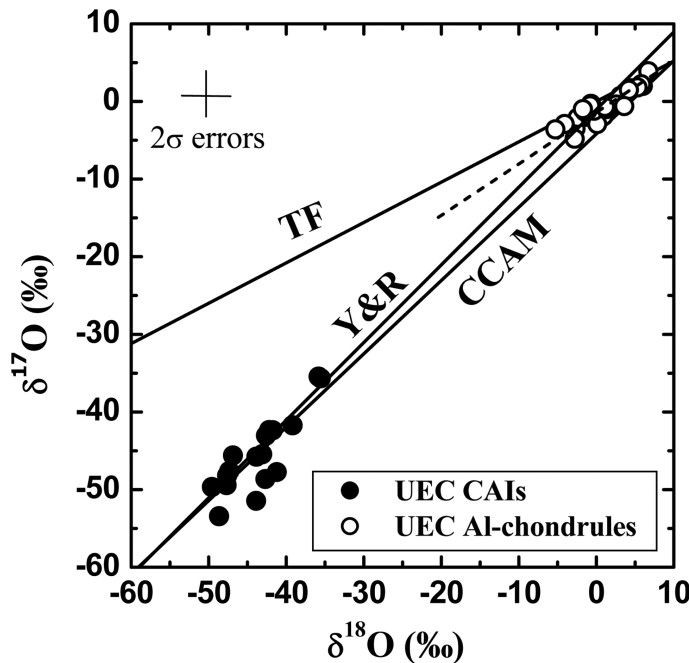


Fig. 5. Oxygen isotopes of aluminum-rich chondrules and CAIs from UECs. Data for UEC CAIs are from Guan et al. (2000b). The dashed line = regression line of aluminum-rich chondrules with a slope of 0.6 ± 0.1 ; TF = terrestrial fractionation line; CCAM = carbonaceous chondrite anhydrous minerals; Y&R = Young and Russell line.

Bulk enstatite chondrites have oxygen isotope compositions that plot close to the terrestrial fractionation line (Clayton et al. 1984; Newton et al. 2000) on a three-oxygen-isotope diagram. Bulk ferromagnesian chondrules from enstatite chondrites fall in a very restricted range along a line of slope 0.7 ± 0.1 (Clayton and Mayeda 1985). Limited in situ measurements of oxygen isotopes of UEC ferromagnesian chondrules (Fagan et al. 2001; Okazaki and Huss 2003) are, in general, consistent with bulk ferromagnesian data from enstatite chondrites (Clayton and Mayeda 1985), albeit with a large scatter. Even though the UEC aluminum-rich chondrules only roughly determine a correlation line of slope $\sim 0.6 \pm 0.1$ (Fig. 3a), similar to the lines defined by bulk ferromagnesian chondrules (slope = 0.7 ± 0.1) (Clayton and Mayeda 1985) or by bulk enstatite chondrites (slope ~ 0.5) (Clayton et al. 1984; Newton et al. 2000), the fact that some of them overlap with ferromagnesian chondrules or fall on the TF line suggest a close relationship between the aluminum-rich and ferromagnesian chondrules in UECs.

The best-fit line to the UEC aluminum-rich chondrule oxygen isotopic compositions does not project through the field of UEC CAIs (Fig. 5) (Guan et al. 2000b; Fagan et al. 2001). This best-fit line also does not correspond to either the slope 0.94 carbonaceous chondrite anhydrous minerals line (CCAM on Fig. 5; Clayton et al. 1997) or the slope 1.0 line of Young and Russell (1998; Y&R on Fig. 5), although the errors on our data do not permit conclusively ruling out the latter. There is also no compelling evidence that the oxygen isotopic compositions of aluminum-rich or ferromagnesian

chondrules in enstatite chondrites might result from mass-dependent fractionation overprinting of a slope ~ 1 mixing line. Therefore, unlike the observation from CR chondrites (Krot et al. 2004), our oxygen isotopic data indicate that the aluminum-rich chondrules in UECs are probably not mixing products of CAIs and ferromagnesian chondrules. Instead, relationships among aluminum-rich chondrules, ferromagnesian chondrules, and CAIs in UECs are similar to those observed in ordinary chondrites (Russell et al. 2000). As is the case with the UOC data, however, additional and more precise data are required to confirm this conclusion.

CONCLUSIONS

Magnesium isotopic systematics have been investigated in eleven aluminum-rich chondrules and two plagioclase fragments from UECs. Only one aluminum-rich chondrule contains clear evidence of in situ decay of ^{26}Al , with an inferred $(^{26}\text{Al}/^{27}\text{Al})_0$ ratio of $(0.68 \pm 0.24) \times 10^{-5}$. The paucity of live ^{26}Al among the UEC aluminum-rich chondrules may result from later metamorphism. However, the widespread occurrence of ^{26}Al -bearing chondrules across the primitive ordinary, carbonaceous, and now enstatite chondrites suggests that the ^{26}Al was widely and at least approximately homogeneously distributed across the chondrite-forming region.

The oxygen isotopic compositions of six UEC aluminum-rich chondrules roughly define a line of slope $\sim 0.6 \pm 0.1$, extending in the ^{16}O -enriched direction from the

ferromagnesian chondrule field of enstatite chondrites. On a three-oxygen-isotope diagram, UEC aluminum-rich chondrules overlap with ferromagnesian chondrules, but are not directly linked to UEC CAIs. These data suggest that, similar to their UOC counterparts, aluminum-rich chondrules in UECs are genetically related to ferromagnesian chondrules and are not hybrid mixtures of ferromagnesian chondrules and CAI material. Similar relationships among aluminum-rich chondrules, ferromagnesian chondrules, and CAIs have also been observed in UOCs (Russell et al. 2000).

Acknowledgments—The manuscript was improved by reviews from S. Mostefaoui, M. Wadhwa, and Associate Editor E. Zinner. We thank the Antarctic Meteorite Working Group and the meteorite curation facility at the NASA Johnson Space Center for providing many of the thin sections used for this study. This work was supported by NASA grants NAG5-11543 (G. R. H.), NAG5-10523 (L. A. L.), NAG5-11809 (L. A. L.), NNG04GK47G (G. J. M.), NAG5-10468 (G. J. M.), and NAG5-12898 (K. M. D.).

Editorial Handling—Dr. Ernst Zinner

REFERENCES

- Bizzarro M., Baker J. A., and Haack H. 2004. Mg isotope evidence for contemporaneous formation of chondrules and refractory inclusions. *Nature* 431:275–278.
- Clayton R. N. and Mayeda T. K. 1985. Oxygen isotopes in chondrules from enstatite chondrites: Possible identification of a major nebular reservoir. 16th Lunar and Planetary Science Conference. pp. 142–143.
- Clayton R. N., Mayeda T. K., and Rubin A. E. 1984. Oxygen isotopic compositions of enstatite chondrites and aubrites. *Journal of Geophysical Research* 89:C245–C249.
- Clayton R. N., Onuma N., Grossman L., and Mayeda T. K. 1997. Distribution of the pre-solar component in Allende and other carbonaceous chondrites. *Earth and Planetary Science Letters* 34:209–224.
- Fagan T. J., McKeegan K. D., Krot A. N., and Keil K. 2001. Calcium-aluminum-rich inclusions in enstatite chondrites (II): Oxygen isotopes. *Meteoritics & Planetary Science* 36:223–230.
- Fahey A. J., Zinner E. K., Crozaz G., and Kornacki A. S. 1987. Microdistributions of Mg isotopes and REE abundances in a type A calcium-aluminum-rich inclusion from Efremovka. *Geochimica et Cosmochimica Acta* 51:3215–3229.
- Grossman J. N. 2004. Loss of chromium from olivine during the metamorphism of chondrites (abstract #1320). 35th Lunar and Planetary Science Conference. CD-ROM.
- Grossman J. N., MacPherson G. J., Hsu W., and Zinner E. K. 1995. Plagioclase-rich objects in the ungrouped E3 chondrite LEW 87234: Petrology and Al-Mg isotopic data (abstract). *Meteoritics* 30:514.
- Guan Y., Huss G. R., and Leshin L. A. 2004a. Further observations of ^{60}Fe - ^{60}Ni and ^{53}Mn - ^{53}Cr systems in sulfides from enstatite chondrites (abstract #2003). 35th Lunar and Planetary Science Conference. CD-ROM.
- Guan Y., Huss G. R., MacPherson G. J., and Leshin L. A. 2002. Aluminum-magnesium isotopic systematics of aluminum-rich chondrules in unequilibrated enstatite chondrites (abstract #2034). 33rd Lunar and Planetary Science Conference. CD-ROM.
- Guan Y., Huss G. R., MacPherson G. J., and Wasserburg G. J. 2000a. Calcium-aluminum-rich inclusions from enstatite chondrites: Indigenous or foreign? *Science* 289:1330–1333.
- Guan Y., Leshin L. A., and MacPherson G. J. 2004b. Oxygen isotopes of aluminum-rich chondrules from unequilibrated enstatite chondrites (abstract #9083). Workshop on Chondrites and the Protoplanetary Disk. CD-ROM.
- Guan Y., McKeegan K. D., and MacPherson G. J. 2000b. Oxygen isotopes in calcium-aluminum-rich inclusions from enstatite chondrites: New evidence for a single CAI source in the solar nebula. *Earth and Planetary Science Letters* 181:271–277.
- Hua X., Huss G. R., Tachibana S., and Sharp T. G. 2005. Oxygen, silicon, and Mn-Cr isotopes of fayalite in the Kaba oxidized CV3 chondrite: Constraints for its formation history. *Geochimica et Cosmochimica Acta* 69:1333–1348.
- Huss G. R. and Lewis R. S. 1990. Interstellar diamonds and silicon carbide in enstatite chondrites. 21st Lunar and Planetary Science Conference. pp. 542–543.
- Huss G. R. and Lewis R. S. 1994. Noble gases in presolar diamonds II: Component abundances reflect thermal processing. *Meteoritics* 29:811–829.
- Huss G. R., MacPherson G. J., Wasserburg G. J., Russell S. S., and Srinivasan G. 2001. ^{26}Al in CAIs and chondrules from unequilibrated ordinary chondrites. *Meteoritics & Planetary Science* 36:975–997.
- Huss G. R., Rubin A. E., and Grossman J. N. Forthcoming. Thermal metamorphism in chondrites. In *Meteorites and the early solar system II*, edited by Lauretta D. and McSween H., Jr. Tucson, Arizona: The University of Arizona Press.
- Jones R. H., Leshin L. A., Guan Y., Sharp Z. D., Durakiewicz T., and Schilk A. J. 2004. Oxygen isotope heterogeneity in chondrules from the Mokoia CV3 carbonaceous chondrite. *Geochimica et Cosmochimica Acta* 68:3423–3438.
- Kita N. T., Nagahara H., Togashi S., and Morishita Y. 2000. A short duration of chondrule formation in the solar nebula: Evidence from ^{26}Al in Semarkona ferromagnesian chondrules. *Geochimica et Cosmochimica Acta* 64:3913–3922.
- Krot A. N. and Keil K. 2002. Anorthite-rich chondrules in CR and CH carbonaceous chondrites: Genetic link between Ca, Al-rich inclusions and ferromagnesian chondrules. *Meteoritics & Planetary Science* 37:91–111.
- Krot A. N., Libourel G., and Chaussidon M. 2004. Oxygen isotopic compositions of the Al-rich chondrules in the CR carbonaceous chondrites: Evidence for a genetic link to Ca-Al-rich inclusions and for oxygen isotope exchange during chondrule melting (abstract #1389). 35th Lunar and Planetary Science Conference. CD-ROM.
- Kunihiro T., Rubin A. E., McKeegan K. D., and Wasson J. T. 2004. Oxygen-isotopic compositions of relict and host grains in chondrules in the Yamato 81020 CO3.0 chondrite. *Geochimica et Cosmochimica Acta* 68:3599–3606.
- LaTourrette T. and Wasserburg G. J. 1998. Mg diffusion in anorthite: Implications for the formation of early solar system planetesimals. *Earth and Planetary Science Letters* 158:91–108.
- MacPherson G. J., Davis A. M., and Zinner E. K. 1995. The distribution of aluminum-26 in the early solar system—A reappraisal. *Meteoritics* 30:365–386.
- MacPherson G. J., Huss G. R., and Davis A. M. 2003. Extinct ^{10}Be in type A calcium-aluminum-rich inclusions from CV chondrites. *Geochimica et Cosmochimica Acta* 67:3165–3179.
- MacPherson G. J. and Huss G. R. 2005. Petrogenesis of Al-rich chondrules: Evidence from bulk compositions and phase equilibria. *Geochimica et Cosmochimica Acta* 69:3099–3127.

- Marhas K. K., Hutcheon I. D., Krot A. N., Goswami J. N., and Komatsu M. 2000. Aluminum-26 in carbonaceous chondrite chondrules (abstract). *Meteoritics & Planetary Science* 35:A102.
- McKeegan K. D., Leshin L. A., Russell S. S., and MacPherson G. J. 1998. Oxygen isotopic abundances in calcium-aluminum-rich inclusions from ordinary chondrites: Implications for nebular heterogeneity. *Science* 280:414–418.
- Mostefaoui S., Lugmair G. W., and Hoppe P. 2005. Fe-60: A heat source for planetary differentiation from a nearby supernova explosion. *The Astrophysical Journal* 625:271–277.
- Newton J., Franchi I. A., and Pillinger C. T. 2000. The oxygen-isotopic record in enstatite meteorites. *Meteoritics & Planetary Science* 35:689–698.
- Okazaki R. and Huss G. R. 2003. Oxygen isotopic composition of individual chondrules in an enstatite chondrite Yamato 791810 (abstract #1791). 34th Lunar and Planetary Science Conference. CD-ROM.
- Rubin A. E., Scott E. R. D., and Keil K. 1997. Shock metamorphism of enstatite chondrites. *Geochimica et Cosmochimica Acta* 61: 847–858.
- Russell S. S., MacPherson G. J., Leshin L. A., and McKeegan K. D. 2000. ^{16}O enrichments in aluminum-rich chondrules from ordinary chondrites. *Earth and Planetary Science Letters* 184: 57–74.
- Russell S. S., Srinivasan G., Huss G. R., Wasserburg G. J., and MacPherson G. J. 1996. Evidence for widespread ^{26}Al in the solar nebula and constraints for nebula time scales. *Science* 273:757–762.
- Sheng Y. J., Hutcheon I. D., and Wasserburg G. J. 1991. Origin of plagioclase-olivine inclusions in carbonaceous chondrites. *Geochimica et Cosmochimica Acta* 55:581–599.
- Srinivasan G., Huss G. R., and Wasserburg G. J. 2001. A petrographic, chemical and isotopic study of calcium-aluminum-rich inclusions and aluminum-rich chondrules from the Axtell (CV3) chondrite. *Meteoritics & Planetary Science* 35:1333–1354.
- Tachibana S. and Huss G. R. 2003. The initial abundance of ^{60}Fe in the solar system. *The Astrophysical Journal* 588:L41–L44.
- Young E. D. and Russell S. S. 1998. Oxygen reservoirs in the early solar nebula inferred from an Allende CAI. *Science* 282:452–455.
- Young E. D., Simon J. I., Galy A., Russell S. S., Tonui E., and Lovera O. 2005. Supra-canonical $^{26}\text{Al}/^{27}\text{Al}$ and the residence time of CAIs in the solar protoplanetary disk. *Science* 308:223–227.